Modeling of Inductive Metal Detector with Swept Frequency Excitation

A.C. Lahrech A. Zaoui F. Benyoubi A. Sakoub

Abstract – **In this paper we present an investigation into using the swept frequency excitation for the inductive metal sensor. The frequency sweep excitation mode allows collecting eddy current data at a wide range of frequencies. The Nyquist polar plot of the sensor response depends on the geometrical and physical proprieties of the detected object. In this work an analytical solution of the response function for the homogenous sphere-shaped is presented. Than a finite element numerical simulation is performed. The swept frequency response is computed for different geometries and metal proprieties.**

1 INTRODUCTION

Landmines, especially Anti-Personnel (AP) mines, are still a worldwide problem. Nowadays a large number of AP mines is buried in the soil. These AP mines kill or cripple around 26 thousand people every year. According to the statistics, half of these victims are civilians, mostly children younger than sixteen years of age.

There are many ways to detect AP mines or buried metal objects in general. Currently, electromagnetic manual methods are still major techniques in detection and clearance. Their main disadvantage is that they are very slow due to many false alarms [1]. Reasons for this failure are especially the variety of environments in which the mines are buried and the limits or flaws of current technology [2].

Excitation signals and signal processing in the detector could be performed in a way to avoid/minimize false alarms. Usage of frequency swept signals is one of these ways. Swept frequency signals give more complex information about the detected objects.

2 PRINCIPLES OF INDUCTIVE METAL DETECTOR

The inductive metal detector usually consists of a search head which contains primary and secondary coils. When the detector passes over an object able to influence the magnetic field it causes a change in the voltage induced in this coil. This influence depends on the electromagnetic and shape properties of the metal object detected.

The inducted voltage is represented by a complex magnitude because the received signal consists of a part which is in phase with the primary signal and a part which is in quadrature with it. Thus, the changes of amplitude and the phase of the received signal contain information about the detected object [3].

The electromagnetic phenomenon in the inductive metal detector is described by the *Ampere's* and *Faraday-Lenz's* law.

The *Ampere's* law is given by:

$$\oint_c B dl = \mu_0 I \tag{1}$$

Where μ_0 is the permeability of vacuum, l is the length of a closed curve.

In accordance with *Faraday-Lenz's law*, eddy currents generate magnetic fields opposed to the primary field. The secondary magnetic field is detected by the receiver coil and induces an electrical voltage in the receive coil according to the *Maxwell-Faraday* equation.

$$\oint_c E dl = -\frac{d\Phi}{dt} \tag{2}$$

Where E is the electric field and Φ is the magnetic flux.

The equation of the *Ampere's* law for a circular coil with radius a can be reformulated using the *Biot-Savart* law. This allows describing the magnetic field at a distance d along the axis of the coil.

$$B = \oint dB_z = \frac{\mu_0}{4\pi} \oint \frac{Idl \cos\Theta}{a^2} \tag{3}$$

After solving the *Biot-Savart* law we get the equation (4), where N is the number of turns of the coil and M is magnetic moment $M=NIS$.

$$B = \frac{N\mu_0 I}{2} \frac{a^2}{\left(r^2 + a^2\right)^{3/2}} = \frac{\mu_0 M}{2\pi\left(r^2 + a^2\right)^{3/2}} \tag{4}$$

The secondary magnetic field depends on many parameters; the depth, orientation, shape, size, electrical conductivity and magnetic permeability of the buried object. It depend also on the EM background and soil properties. The frequency of the primary magnetic field is very important as it influences substantially the depth of eddy currents penetration. A low-frequency magnetic field penetrates deeper into the ground, is less affected by the ground effect [4] and the skin effect is reduced.

On the other hand high frequencies offer better resolution. The dependence of detection properties on the frequency of the exciting electromagnetic field

Laboratoire Systèmes Electromagnétiques, Ecole Militaire Polytechnique, BP17, 16111 Bordj El Bahri, Algiers, Algeria.
e-mail: zaoui_abdelhalim@yahoo.fr

978-1-4673-5707-4/13/$31.00 ©2013 IEEE

opens the opportunity to develop new methods of primary coil excitation and signal processing of the received signal with the intention to better identify geometry, depth and material of the buried object.

3 ELECTROMAGNETIC MODELLING

We present in this section the model of the electromagnetic sensor when using an homogenous sphere target as shown in Figure 1. the sensor is constituted of separated transmitting and receiving coils with operating frequency ω. The homogeneous sphere with radius a, conductivity σ and permeability μ is used as a target. The transmission coil is placed between two receiving coils. These last are operating in differential mode. All the coil in this sensor are in the same axis.

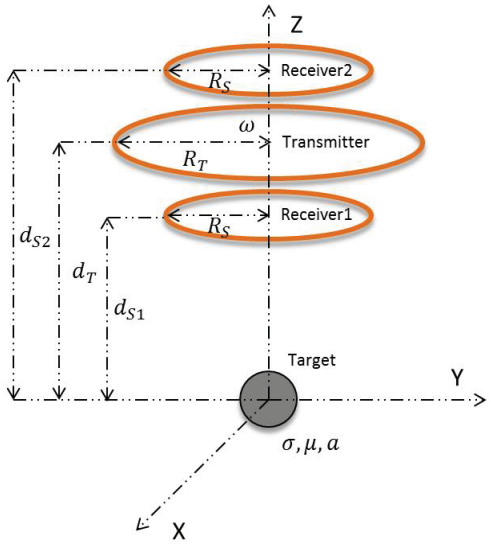

Figure 1: Model of coaxial coils in the axis of a homogenous sphere.

For this model we can define the response [5] V_s as:

$$V_s = 2\pi j\mu_0 I\omega\left(\frac{a^3}{4}\right)\frac{{R_T}^2{R_S}^2}{\left({d_T}^2+{R_T}^2\right)^{3/2}} \times\left[\frac{1}{\left({d_{S2}}^2+{R_S}^2\right)^{3/2}}-\frac{1}{\left({d_{S1}}^2+{R_S}^2\right)^{3/2}}\right] \times\left[X(ka)+jY(ka)\right] \quad (5)$$

Where μ is the permeability, I is the current driven by the coil, ω is the operating frequency, R_T is the radius of the transmitting coil, d_T is the distance of the coil from the target, R_S is the radius of two receiving coils, d_{S1} is the distance of receiver1 coil from the target. d_{S2} is the distance of receiver2 coil from the target.

The term $X(ka)+jY(ka)=F(\alpha)$ depends on the frequency, permeability, conductivity and radius of the target. The response parameter α is given by :

$$j\alpha = j\omega\mu\sigma a^2 = 2j\frac{a^2}{\delta^2} \quad (6)$$

The variable α depends on object parameters (also on depth of penetration). The dependency of the imaginary part of the response function on the response parameter is shown in Figure 2. For more detail, see [5].

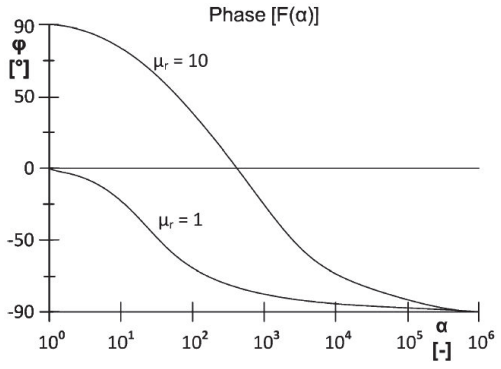

Figure 2: Response function of ferromagnetic (μ_r = 10) and non-ferromagnetic (μ_r = 1) object [2].

4 NUMERICAL ANALYSIS METHOD

The numerical model is obtained by finite element resolution of the magneto-dynamic diffusion equation given by [6]:

$$\vec{\nabla}\times\left(\frac{1}{\mu}\vec{\nabla}\times\vec{A}\right)+\sigma\frac{\partial\vec{A}}{\partial t}=\vec{J}_s \quad (7)$$

Where μ, σ, J_s and A are respectively the magnetic permeability, the electric conductivity, the source current density and magnetic vector potential. Applying the finite-element formulation for space, the following type of matrix equation is obtained:

$$[S]\{A\}+[C]\left\{\frac{\partial A}{\partial t}\right\}=\{Q\} \quad (8)$$

The matrix C is an appropriately sized constant matrix associated both with the eddy-current regions in the magnetic field and energy-storage elements such as inductors and capacitors in the electric circuit. The coefficient matrix S in general is a constant in linear systems. The right-hand column matrix Q is

associated with excitations such as voltage sources and current sources [7].

The time variable in (8) can be discretized using backward Euler method. The recursive formula of (8) when using the backward Euler method is:

$$[S]\{A^n\}+[C]\left\{\frac{A^{n+1}-A^n}{\Delta t}\right\}=\{Q\} \qquad (9)$$

Where $\{A\}^n$ is the magnetic potential evaluated at time t^n end the time step size $\Delta t = t^{n+1} - t^n$.

Equation (9) is solved by using time-stepping method in the time domain. According to (9), at each time step, the following algebraic matrix equation is solved:

$$\left[\frac{1}{\Delta t}[C]+[S]\right]\{A\}^{n+1}=\{Q\}^{n+1}+\frac{1}{\Delta t}[C]\{A\}^n \qquad (10)$$

The response signal in inductive metal detector is the electromotive force induced in the sensor receiving coils, calculated as follows:

$$V_{emf}=\frac{\{A\}^{n+1}-\{A\}^n}{\Delta t}2\pi r_c \qquad (11)$$

Where r_c is the centroidal radius of a coil element.

5 SIMULATION RESULTS.

This section is dedicated to the presentation of the simulation results. Figure 3 present the plot of the magnetic equipotential. The parameters of the metal detector are given in Table I. The transmitting coil is excited by a step sweep sinus signal from 1 kHz to 45 kHz with a step of 1 kHz and amplitude of 12 V. The operating frequency f sweeps linearly form f_1 to f_2 as shown in figure 4.

For the numeric simulation, spheres of different sizes and materials were used. All spheres were placed at distance of 100 mm from the coils in the open air. The spheres were not placed into the ground to avoid the ground effect [4]. All targets were placed on the axis of the greatest sensitivity of the receiving coil and the frequency dependence of the response function was measured.

The polar plot of the sensor response for different sizes of ferromagnetic steel sphere is presented in Figure 5. The differences between the amplitude spectra are noticeable on higher frequencies. In other hand, the phase shift increases significantly with the size.

In Figure 6, the responses of ferromagnetic steel and non-ferromagnetic copper with 20mm diameters are presented. These responses confirm that there is a significant difference between the two material responses.

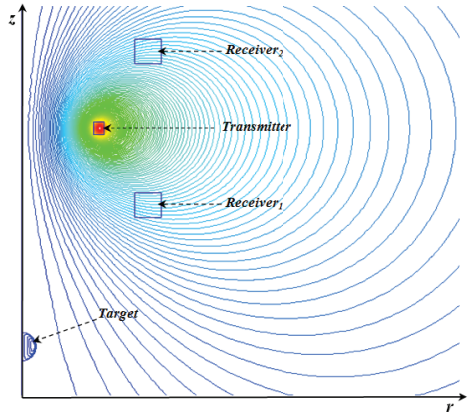

Figure 3: Flux lines of inductive metal detector. System is axisymmetrical around the *z*-axis.

Parameter	Value
Inner diameter of the transmitter coil	100 mm
Inner diameter of the receiver coils	158 mm
Number of layer of the transmitter coil	9
Number of layer of receiver coils	37
Number turns per layer of the transmitter coil	7
Number turns per layer of the receiver coils	35
Height of the transmitter coil	9 mm
Height of the receiver coils	17.5 mm
Width of the transmitter coil	7 mm
Width of the receiver coils	18.5 mm
Diameter of copper wire of the transmitter coil	1 mm
Diameter of copper wire of the receiver coils	0.5 mm
Distance between the coils	55 mm

Table 1: Parameters of inductive metal detector.

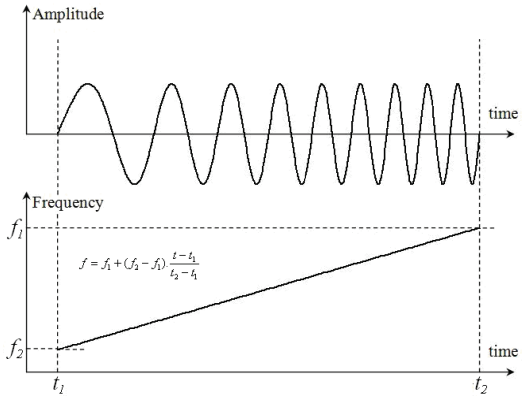

Figure 4: Linear frequency sweep.

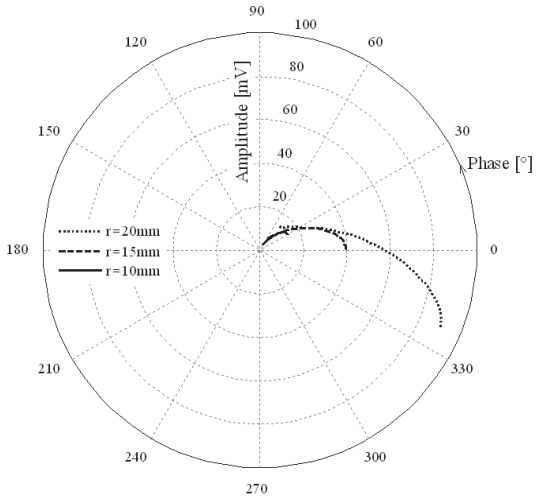

Figure 5: Polar response plot for Steel.

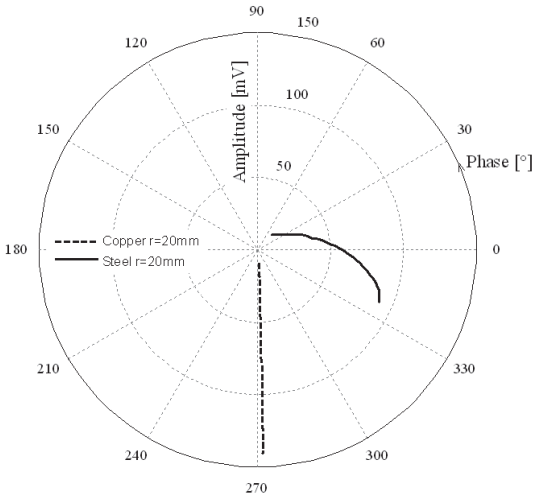

Figure 6: Polar response plot for Copper and Steel.

3 CONCLUSION

In this work an analysis of an electromagnetic inductive sensor response of the homogenous sphere target was done, as well as measured numerical data from different objects. For data processing FFT methods were used. Frequency sweep signal, as a source of a transmitting coil, bring a different approach for distinguishing between objects. Based on this analyze we conclude that the better outline of the object in terms of geometric and electromagnetic properties (conductivity, permeability) can be obtained when the detector excitation is done by a frequency sweep signal. The Nyquist polar plot of the sensor response can be considered as a signature of the target.

References

[1] John Wayne Brooks "The Detection of Buried Non-Metallic Anti-Personnel Land Mines" Research Reports, University of Alabama in Huntsville, 2000.

[2] J. Svatos, J. Vedral, and P. Fexa, "Metal detector excited by frequency swept signals," Metrol. Meas. Syst., vol. XVIII, no. 1, pp. 57–68, 2011.

[3] J. Svatos, J. Vedral, "The Usage of Frequency Swept Signals for Metal Detection," *IEEE Trans. Magn*., vol. 48, no. 4, pp. 1501–1504, Apr. 2012.

[4] C. Bruschini, "On the low frequency EMI response of coincident loops over a conductive and permeable soil and corresponding background reduction schemes," *IEEE Trans. Geosci*. Remote Sens., vol. 42, no. 8, pp. 1706–1719, Aug. 2004.

[5] C. Bruschini, "A multidisciplinary analysis of frequency domain metal detectors for humanitarian demining," Ph.D. dissertation, Faculty Appl. Sci., Vrije Univ., Brussels, Belgium, 2002.

[6] S. Xie, Z. Chen, T. Takagi, and T. Uchimoto, "Efficient Numerical Solver for Simulation of Pulsed Eddy-Current Testing Signals," *IEEE Trans. Magn*., vol. 47, no. 11, pp. 4582–4591, Nov. 2011.

[7] W. N. Fu, Xiu Zhang, and S. L. Ho, "A Fast Algorithm for Frequency-Domain Solutions of Electromagnetic Field Computation of Electric Devices Using Time-Domain Finite-Element Method," *IEEE Trans. Magn*., vol. 49, no. 1, pp. 530–535, Jan. 2013.